TECHNICAL REPORT NO. 10278

ANALYSIS OF SOIL INDENTATION BY A TRANSLATING GROUSER PLATE

October 1968

by

J. L. DAIS
LAND LOCOMOTION DIVISION

TACOM

MOBILITY SYSTEMS LABORATORY

U.S. ARMY TANK AUTOMOTIVE COMMAND Warren, Michigan

DISCLAIMER NOTICE

THIS DOCUMENT IS BEST QUALITY PRACTICABLE. THE COPY FURNISHED TO DTIC CONTAINED A SIGNIFICANT NUMBER OF PAGES WHICH DO NOT REPRODUCE LEGIBLY.

TECHNICAL REPORT NO. 10278

ANALYSIS OF SOIL INDENTATION BY A TRANSLATING GROUSER PLATE

By

J. L. Dais

October 1968

AMCMS CODE: 5535.12.426

ACKNOWLEDGEMENT

The results reported herein were in part obtained during the course of summer employment with the Land Locomotion Division of the U.S. Army Tank-Automotive Command

ABSTRACT

Soil is idealized as a weightless isotropic frictional material with cohesion, and quasi-static solutions are obtained to the two-dimensional problems of indentation by a plate with a single spud and an infinitely long plate with equally spaced spuds of uniform depth.

TABLE OF CONTENTS

LIST OF FIGURES

OBJECT:

The object here is to analytically investigate the action of grouser plates under applied load. The grouser plate of Figure 1 simulates a weapon spade and that in Figure 9 a bulldozer track. It will be attempted to obtain solutions in a form which can be interpreted by a designer in selecting an optimum plate geometry.

INTRODUCTION:

The problem of initial indentation of a half-space of soil by a rigid translating grouser plate will be considered as a two dimensional problem as shown in Figure 1. The plate can be taken to translate at angle θ to the horizontal; the essential analytical result is then the magnitude P and the line of action of the corresponding collapse load. Alternatively, the problem can be considered as having the inclination σ of the collapse load specified; P and θ are then the essential results. For definiteness in limiting the scope of the paper, solutions will not be considered for $\theta \geq \frac{\pi}{2}$.

The specification of descriptive and yet analytically simple plate-soil interface conditions for this problem is tricky and reflects judgment based to some extent on experimental and field experience. The interface is here taken to be perfectly rough unless the solution involves separation there (as in Figure 6(a)), in which case the traction vector is taken to vanish. Thus, the solution will in part determine the interface condition.

Bekker (1) stressed the practical importance of developing ground failures rather than grip failures in land locomotion. If θ is large in Figure 1, then the situation corresponds to what Bekker termed "ground" failure. If θ is sufficiently negative, then the situation corresponds to what Bekker termed "grip" failure. Deformed configurations for $\theta = -25^\circ$ and $+10^\circ$ corresponding to equal amounts of plate displacement are shown respectively in Figures 6(a) and 6(b). In Figure 6(a) the plate has lifted, and thus it is a smaller section which remains to be failed. Furthermore, the deformation is concentrated on a plane leading to the free surface. It is likely that failure (i.e. the complete splitting away of a soil mass translating rigidly with the plate) would occur at a much smaller plate displacement in an experiment or a field situation described by Figure 6(a) as contrasted with Figure 6(b).

This analysis takes the soil parameters cohesion and internal friction to be constants and neglects soil weight, end effects of the grouser plate, and soil flow out of the plane. Plate end effects become important in situations where the grouser width/depth ratio is not large. Soil weight is important in this problem if the soil is cohesionless, and also if the soil has cohesion and the grouser depth is large.

Inclusion of these effects would lead to larger loads so their neglect here could be thought of as lending an analysis on the safe side. Soil flow out of the plane becomes important in situations where the plate length/width ratio is substantial and flow can occur at an almost vertical load. A practical example of this is the tracked vehicle problem where soil bearing capacity does not substantially exceed the vehicle weight. The inclusion of this effect would lead to a smaller collapse load.

Plates are frequently designed with curved or inclined grousers as shown in Figure 2. Provided that the back face of the grouser does not approach the soil behind the plate, the present analysis is applicable. The essential plate parameters here are OD and $\prec$E O D$\succ$ as shown in the figure.

Two dimensional indentation by an infinitely long rigid plate with equally spaced grousers is considered as in Figure 9. For this problem material incompressibility prevents plate displacements with $\theta > 0$. Corresponding to a given value of δ, distinct values Q of collapse load/unit plate length will be found. Until experiment dictates otherwise, it seems reasonable to conjecture that the solution to which there corresponds the smallest value of Q would be most descriptive of field situations.

THE GOVERNING EQUATIONS:

For a frictional material (2), the stress state is taken to obey the Coulomb limit condition; i.e. on no surface is the magnitude τ of the shear stress vector allowed to exceed $c - \sigma_N \tan\phi$, where c is cohesion and $\tan\phi$ and σ_N are respectively the friction coefficient and normal stress on a surface. Expressed alternatively, the Mohr's circle defined by σ_1 and σ_3, respectively the algebraically greatest and least principal stress components, must lie inside of or just touch the Coulomb line of Figure 3(a). If the circle touches the envelope, then as indicated by Figures 3(a) and 3(b), the equation

$$(\sigma_x+\sigma_y)\sin\varphi + \left\{(\sigma_x-\sigma_y)^2 + 4\tau_{xy}^2\right\}^{\frac{1}{2}} = 2c\cos\varphi \qquad (1)$$

holds, where x and y axes are taken in the plane of σ_1 and σ_3. In the absence of body force, the equations of plane equilibrium are

$$\left.\begin{aligned} \frac{\partial \sigma_x}{\partial x} + \frac{\partial \tau_{xy}}{\partial y} &= 0 \\ \frac{\partial \tau_{xy}}{\partial x} + \frac{\partial \sigma_y}{\partial y} &= 0 \end{aligned}\right\} \qquad (2)$$

The equations (1) and (2) can be transformed into a system of two first order quasilinear hyperbolic differential equations with characteristics, usually termed α lines and β lines, inclined at $-(\frac{\pi}{4} + \frac{\phi}{2})$ and $+(\frac{\pi}{4} + \frac{\phi}{2})$ to the direction of σ_1.

If ψ denotes the angle of inclination of the direction of σ_1 to the x-axis as shown in Figure 4, and $-\frac{1}{2}(\sigma_x + \sigma_y)$ is denoted by

$$p = -\frac{1}{2}(\sigma_x + \sigma_y), \qquad (3)$$

then the state of stress is determined by p and ψ whereever equation (1) holds, and the characteristic equations

$$\cot \varphi \, dp + 2(p + c \cot \varphi) d\psi = 0 \qquad (4)$$

and

$$\cot \varphi \, dp - 2(p + c \cot \varphi) d\psi = 0 \qquad (5)$$

must hold on α and β lines respectively.

The material is rigid if the circle in Figure 3(a) does not touch the envelope. If the circle touches the envelope, then deformation can occur by plane strain in the plane of σ_1 and σ_3 either by a tangential jump of velocity across an α or β line or with zero volume change by a continuous velocity field in which the direction of algebraically greatest principal strain rate, $\dot{\varepsilon}_1$, is inclined at either $-\frac{\phi}{2}$ or $+\phi/2$ to the direction of σ_1. The velocity equations corresponding to either of these inclinations are a system of two first order linear hyperbolic equations; for the former inclination the α line is one characteristic and the line orthogonal to the α line, termed a γ line, is a second characteristic; for the latter the β line is one characteristic and the line orthogonal to the β line, termed a ρ line, is a

second characteristic. The characteristic curves are shown in Figure 4. If v_α , v_β , v_ρ , and v_γ denote the projection of the velocity vector on the corresponding characteristic line, then in the former case

$$dv_\gamma + v_\alpha d\Psi = 0 \tag{6}$$

and

$$dv_\alpha - v_\gamma d\Psi = 0 \tag{7}$$

must be satisfied on γ and α lines respectively; in the latter case

$$dv_\beta + v_\rho d\Psi = 0 \tag{8}$$

and

$$dv_\rho - v_\beta d\Psi = 0 \tag{9}$$

must be satisfied on β and ρ lines respectively.

ANALYSIS OF THE SINGLE SPUD PROBLEM:

Solutions exhibited will consist of the stress characteristic fields of Figures 5*(a)-(d), solutions of equations (4) and (5), and velocity fields which satisfy equations (6)-(9) where they are continuous and take a tangential jump across and α or β line where they are discontinuous. The velocity solutions, if maintained during a small plate displacement, will distort initially square grids as shown in Figures 6(a)-(d). The regions outside of the characteristic field of Figures 5(a)-(d) are taken to be rigid. A collapse load will be associated with the stress fields.

The introduction of the variables ξ , θ , and ℓ of Figure 5 will facilitate the analysis. The inclination to the horizontal of the α line which intersects the point D is denoted by θ . $\angle$ EOD$>$ in Figures 5(b)-(d) is denoted by ξ ; in Figure 5(a) the inclination to the plate of the α line which intersects the point D is denoted by ξ ; the point of intersection with the plate is labelled as A . OD in Figures 5(b)-(d) is denoted by ℓ ; in Figure 5(a) the length of the α which intersects the point D is denoted by ℓ . An expression

*The stress characteristic field of Figure 5(b) was proposed by Haythornthwaite (3)

for the collapse load will be obtained which will equilibrate the uniform stress states along the lines AD of Figure 5(a) and OD of Figures 5(b)-(c).

For plates with $< EOD >$ sufficiently small (if $\varphi = 30^{\circ}$, then $< EOD >$ cannot exceed about 36°) the characteristic field of Figure 5(c) can be constructed with $< BOD > = < CDG >$. For $< EOD >$ in this range, one of the fields of Figures 5(a), (b), or (c) will be appropriate depending on σ and $< EOD >$. Otherwise one of the fields of Figures 5(b), (c), or (d) is appropriate depending on σ and $< EOD >$.

An equation which relates θ to $< EOD >$ in Figure 5(c) can be obtained by equating the length of ED to $\ell \sin < EOD >$ and also to the length of FD times $\sin(2\theta - \varphi - \frac{\pi}{2})$. There results the expression

$$\sin(\tfrac{\pi}{2} - \varphi)\sin< EOD > =$$

$$2\sin(2\theta-\varphi-\tfrac{\pi}{2})\cos(\tfrac{\pi}{4} - \tfrac{\varphi}{2})\sin(\tfrac{\pi}{2} +\varphi -< EOD >-\theta)e^{(\frac{\pi}{4} - \frac{\varphi}{2} +\theta)\tan\varphi}.$$

It follows from trigonometric identities that

$$\tan(\theta-\varphi) - \frac{\cos\varphi\, e^{-(\frac{\pi}{4} - \frac{\varphi}{2} +\theta)\tan\varphi}}{2\cos(2\theta-\varphi)\cos(\tfrac{\pi}{4} - \tfrac{\varphi}{2})\cos(\theta-\varphi)} = \cot < EOD >. \qquad (10)$$

For sufficiently small $< EOD >$, equation (10) will have a solution for θ.

A pressure distribution which satisfies equations (4) and (5) in the fields of Figures 5(b)-(d) is

$$p = \frac{c\cos\varphi}{(1-\sin\varphi)} \qquad \text{in OAB,}$$

$$p = c\cot\varphi\left[\frac{e^{2(\frac{\pi}{4} - \frac{\varphi}{2} +\theta-\mu)\tan\varphi}}{(1-\sin\varphi)} - 1\right] \qquad \text{in OBC,}$$

$$\text{and} \quad p = c\cot\varphi\left[\frac{e^{2(\frac{\pi}{4} - \frac{\varphi}{2} +\theta)\tan\varphi}}{(1-\sin\varphi)} - 1\right] \qquad \text{in OCDE.} \qquad (11)$$

Equation (11) holds also in EAD of Figure 5(a).

If the characteristic field of Figure 5(b) applies, then a velocity solution for which the perfectly rough plate translates with speed V at angle $\Theta = \theta$ to the x-axis is

$$\left.\begin{aligned} v_\alpha &= V \\ v_\gamma &= 0 \end{aligned}\right\} \text{ in OCDE,} \qquad (12)$$

$$\left.\begin{aligned} v_\alpha &= Ve^{-(\frac{\pi}{4} - \frac{\varphi}{2} + \theta)\tan\varphi} \\ v_\gamma &= 0 \end{aligned}\right\} \text{ in OAB,}$$

$$\left.\begin{aligned} \text{and } v_\beta &= -V \sin\varphi\, e^{-\mu \tan\varphi} \\ v_\rho &= V \cos\varphi\, e^{-\mu \tan\varphi} \end{aligned}\right\} \text{ in OBC.}$$

Equation (12) also applies to region EAD of Figure 5(a). The velocity vector experiences a tangential jump across the α line intersecting the point D.

A velocity solution valid for $\theta \leq \Theta < \frac{\pi}{2}$ corresponding to the field of Figure 5(c) is

$$\left.\begin{aligned} v_\alpha &= V \cos(\Theta - \theta) \\ v_\gamma &= -V \sin(\Theta - \theta) \end{aligned}\right\} \text{ in OCDE,}$$

$$\left.\begin{aligned} v_\beta &= -V \tan\varphi \cos(\Theta - \theta + \varphi) e^{-\mu \tan\varphi} \\ v_\rho &= V \cos(\Theta - \theta + \varphi) e^{-\mu \tan\varphi} \end{aligned}\right\} \text{ in OBC,}$$

$$v_\alpha = \frac{V}{\cos\varphi}\cos(\Theta - \theta + \varphi)e^{-(\frac{\pi}{4} - \frac{\varphi}{2} + \theta)\tan\varphi}$$

$$v_\gamma = 0$$

} in OAB,

$$v_\alpha = -V\tan\varphi\sin(\Theta - \theta)e^{-\mu'\tan\varphi}$$

$$v_\gamma = V\sin(\Theta - \theta)e^{-\mu'\tan\varphi}$$

} in DCG,

and $$v_\beta = -\frac{V}{\cos\varphi}\sin(\Theta - \theta)e^{-(\frac{\pi}{4} - \frac{\varphi}{2} + \theta)\tan\varphi}$$

$$v_\rho = 0$$

} in FEDG.

The velocity vector undergoes a tangential jump across the curves FGC, CBA, DC and CO, and the region translates with the zone FGD.

If the stress field of Figure 5(d) applies, then a velocity solution valid for $< EDO > + \varphi \leq \Theta < \frac{\pi}{2}$ is

$$v_\alpha = V\cos(\Theta - < EDO > - \varphi)$$

$$v_\gamma = -V\sin(\Theta - < EDO > - \varphi)$$

} in OCE,

$$v_\beta = -V\tan\varphi\cos(\Theta - < EDO >)e^{-\mu\tan\varphi}$$

$$v_\rho = V\cos(\Theta - < EDO >)e^{-\mu\tan\varphi}$$

} in OAB,

and $$v_\alpha = \frac{V}{\cos\varphi}\cos(\Theta - < EDO >)e^{-(\frac{\pi}{4} + \frac{\varphi}{2} + < EDO >)\tan\varphi}$$

$$v_\gamma = 0$$

} in OBC.

Tangential jumps in velocity occur across CBA and CO.

Figure 7 will facilitate the determination of the magnitude P and inclination δ of the corresponding plate collapse load. The inclination $(\delta - \xi)$ of the plate collapse load to $\underline{n}$ is the same as the inclination of the stress vector on OD to $\underline{n}$ and the magnitude P of the load is ℓ times the magnitude of the stress vector. It follows from Figure 7(b) and equation (11) that

$$\tau_{\zeta\eta} = R \cos(2\theta + 2\xi - \varphi) = P/\ell \sin(\delta - \xi) , \tag{13}$$

$$-\sigma_{\eta\eta} = [p + R \sin(2\theta + 2\xi - \varphi)] = P/\ell \cos(\delta - \xi) \tag{14}$$

where

$$R = c \cos \varphi \left[\frac{e^{2(\frac{\pi}{4} - \frac{\varphi}{2} + \theta)\tan \varphi}}{(1 - \sin \varphi)} \right] \tag{15}$$

and

$$P/R = \frac{1 - (1 - \sin \varphi) e^{-2(\frac{\pi}{4} - \frac{\varphi}{2} + \theta)\tan \varphi}}{\sin \varphi} . \tag{16}$$

From equations (13), (14), and (16) there follows

$$\cot(\delta - \xi) = \frac{1}{\cos(2\theta + 2\xi - \varphi)} \left[\sin(2\theta + 2\xi - \varphi) + \frac{1 - (1 - \sin\varphi) e^{-2(\frac{\pi}{4} - \frac{\varphi}{2} + \theta)\tan \varphi}}{\sin \varphi} \right] \tag{17}$$

$$P/\ell c = \frac{\cos(2\theta + 2\xi - \varphi) \cos \varphi}{\sin(\delta - \xi)(1 - \sin \varphi)} e^{2(\frac{\pi}{4} - \frac{\varphi}{2} + \theta)\tan \varphi} \quad \text{if} \quad \delta \neq \xi , \tag{18}$$

and

$$P/\ell c = \frac{\cos\varphi}{\cos(\delta-\xi)}\left[\frac{e^{2(\frac{\pi}{4}-\frac{\varphi}{2}+\theta)\tan\varphi}}{(1-\sin\varphi)}\right]\left[\sin(2\theta+2\xi-\varphi)+\frac{1-(1-\sin\varphi)e^{-2(\frac{\pi}{4}-\frac{\varphi}{2}+\theta)\tan\varphi}}{\sin\varphi}\right] \quad \text{if} \quad \delta \neq \xi+\frac{\pi}{2}\,. \tag{19}$$

PLATE PERFORMANCE CURVES:

For applications, equations (10), (17), (18), and (19) can be conveniently represented by plate performance curves. For $\varphi = 30^\circ$ (a reasonable value of φ) Figure 8 shows such curves for $\xi = 0^\circ$, 15°, 30°, 45°, 60°, 75°, and 90°, and their use in performance prediction of plates with $<\text{EOD}> = 0^\circ$, 15°, 30°, 45°, 60°, 75°, or 90° will be explained. Plates with other values of $<\text{EOD}>$ can be treated by interpolating between the curves.

If σ is given, then ordinarily the curve for $\xi = <\text{EOD}>$ will associate values of θ and $P/\ell c$ with σ. If σ is so small that the curve for $\xi = <\text{EOD}>$ is not touched by a vertical line from σ, then the plate will translate with $\theta > \frac{\pi}{2}$, the situation thus being outside the scope of the present paper. If σ is so large that the curve for $\xi = <\text{EOD}>$ is not reached, then θ and $P/\ell c$ can be obtained using the dotted curves; $<\text{EAD}>$ of Figure 6(a) is then equal to θ.

If θ is given, then ordinarily the curve for $\xi = <\text{EOD}>$ will associate values of σ with θ. If θ is so small that the curve for $\xi = <\text{EOD}>$ is not reached by a horizontal line from θ, then the dotted line will associate a value of σ with θ; $<\text{EAD}>$ of Figure 6(a) is then equal to θ. In either case, $P/\ell c$ can then be determined from σ as in the preceding paragraph.

ANALYSIS OF THE INFINITE PLATE PROBLEM:

In Figure 9, if σ is sufficiently small (less than about 25° if $\varphi = 30^\circ$), the plate will not displace. For larger values of σ three alternative solutions are exhibited. The stress characteristic fields for these solutions are shown in Figures 10(a)-(c), where t in Figures 10(a) and 10(b) is arbitrary. If the pressure is an arbitrary

constant in these fields, then equations (4) and (5) are satisfied. The solution corresponding to Figure 10(c) requires $-\theta> < EOD >$ by an amount sufficient so that the region DAOB can support the required traction along AD . A collapse load will be assigned to each of the stress fields.

Take the plate to translate with speed V. Then a velocity solution corresponding to Figure 10(a) for which the region above α_1 translates with speed V at $\Theta = 0$ is

$$\left.\begin{aligned} v_\gamma &= 0 \\ v_\alpha &= \frac{V s_\gamma}{t} \end{aligned}\right\}$$

between α_0 and α_1 , where s_γ denotes distance along a γ line from α_0 . The region below α_0 is taken rigid. A velocity solution corresponding to Figure 10(b) for which the region above ρ_1 translates with speed V at $\Theta = 0$ is

$$\left.\begin{aligned} v_\beta &= 0 \\ v_\rho &= \frac{V s_\beta}{t} \end{aligned}\right\}$$

between ρ_0 and ρ_1 , where s_β denotes distance along a β line from ρ_0 . The region below ρ_0 is taken rigid. These velocity solutions maintained through a small displacement would distort a grid of initially vertical lines as is shown in Figure 11(a). A velocity solution corresponding to Figure 10(c) for which the region above α_0 translates with speed V at $\Theta = \Theta$ is

$$\left.\begin{aligned} v_\alpha &= V \\ v_\alpha &= 0 \end{aligned}\right\}$$

above α_0 . The velocity vector experiences a tangential jump across α_0 and the region below α_0 remains rigid. This velocity solution

maintained through a small displacement would distort a grid of initially vertical lines as is shown in Figure 11(b).

A collapse load can quite simply be assigned to the characteristic field of Figure 10(a) by noting that $\tau = c - \sigma_N \tan \varphi$ on α lines. It then follows from $\tau = Q \sin \delta$ and $\sigma_N = - Q \cos \delta$ that

$$Q/c = \frac{1}{\sin \delta - \cos \delta \tan \varphi} . \qquad (20)$$

For the case $\varphi = 30^\circ$ this equation is exhibited graphically in Figure 12. It follows readily from the Mohr diagram of Figure 3(a) that $(1 + 2 \tan^2 \varphi)\tau = c - \sigma_N \tan \varphi$ on β lines. Then from $\tau = Q \sin \delta$ and $\sigma_N = -Q \cos \delta$ it follows that

$$Q/c = \frac{1}{\sin \delta (1 + 2 \tan^2 \varphi) - \cos \delta \tan \varphi} \qquad (21)$$

corresponds to Figure 10(b). This equation is also exhibited graphically in Figure 12 for the case of $\varphi = 30^\circ$. It follows from the geometry of Figure 10(c) that $\ell/L = \tan \langle EOD \rangle / \sin \theta$. The results of the previous sections are applicable to find θ and $P/\ell c$; the collapse load is then given by

$$Q/c = \frac{\sin \langle EOD \rangle}{\sin \theta} [P/\ell c] . \qquad (22)$$

For the case $\varphi = 30^\circ$ and plates with $\langle EOD \rangle = 4^\circ$, 7°, and 10° the plate performance curves of Figure 8 were used to exhibit equation (22) graphically in Figure 12.

Bekker (1) analyzed this problem previously and obtained a collapse load equivalent to the one obtained here corresponding to Figure 10(a). As was discussed by Bekker (3), (4), this solution implies that the drawbar pull of tracked vehicles should be independent of spud depth and spud spacing. The solutions obtained here have the following implications for track design: As long as $\langle EOD \rangle$ is greater than roughly 8° of 10° then drawbar pull is independent of $\langle EOD \rangle$. However, for lesser values of $\langle EOD \rangle$ significant reductions of drawbar pull can result from decreasing $\langle EOD \rangle$. Such reductions would occur only in terrains of reasonably high strength soil.

CONCLUSIONS:

It is the opinion of the author that the solutions obtained for the plate with the single spud are sufficiently descriptive of field situations involving weapon spades that useful implications for spade design can be deduced.

The infinitely long plate problem, however, involves a troublesome nonuniqueness of solution, as is indicated in Figure 12. For sufficiently small inclinations of the collapse load to the horizontal, three solutions have been obtained, each having a distince collapse load magnitude. For steeper inclinations, two solutions have been obtained, each with a distinct collapse load magnitude. It appears likely to the author that the solutions with the lowest load magnitude will best correlate with field situations. This, however, is a matter which would be more satisfactorily approached by experiment than conjecture.

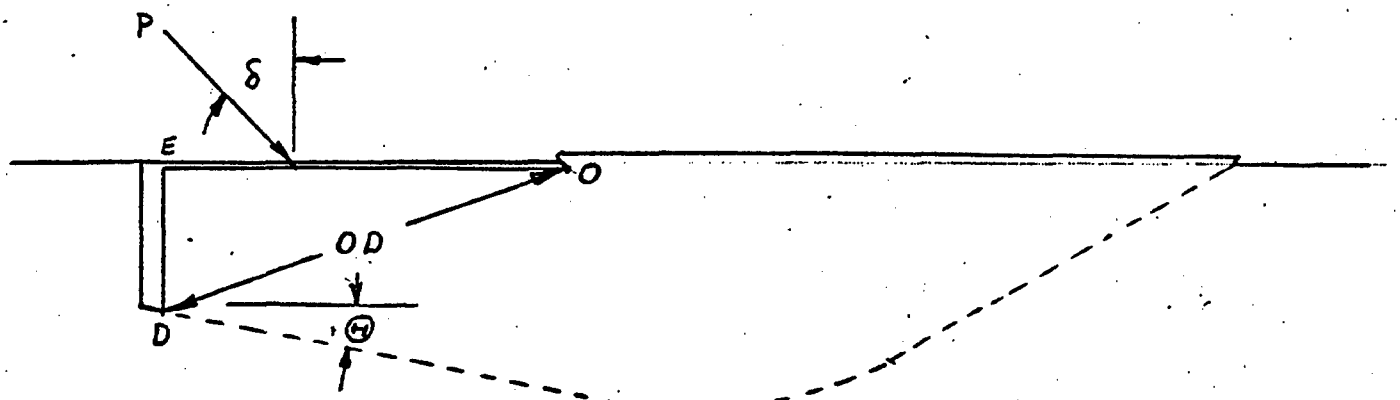

Figure 1. Configuration of plate and soil before and after small indentation. Soil below the dashed curve has remained rigid. OD and < EOD > are the essential plate parameters.

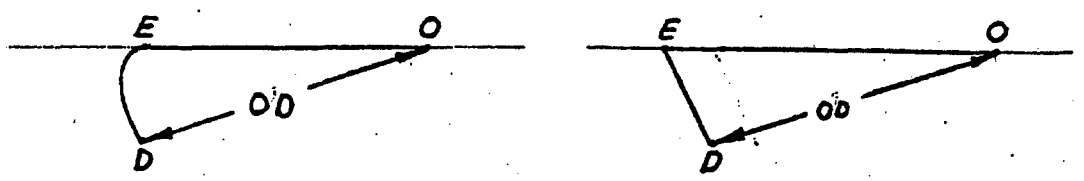

Fig. a Fig. b

Figure 2. Plates with Curved or Inclined Grousers

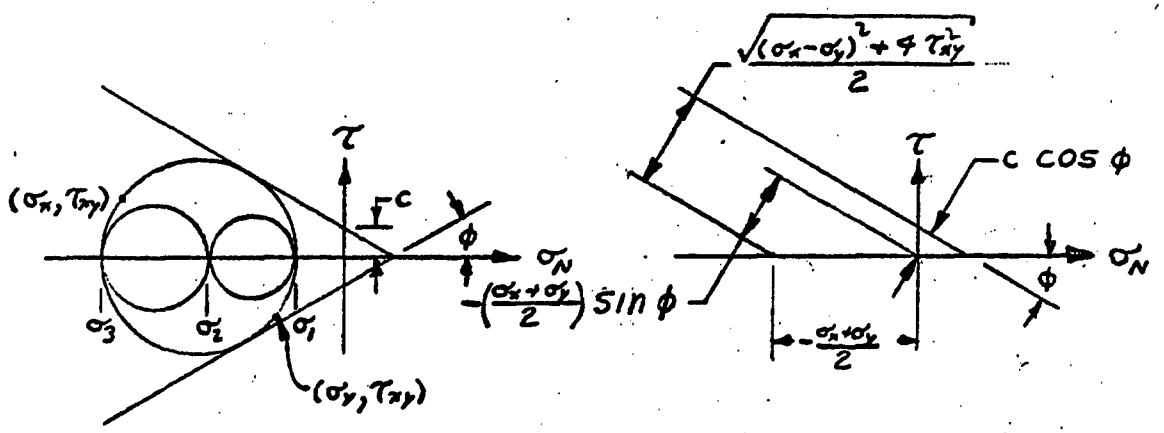

Fig. a Fig. b

Figure 3. The Coulomb Yield Condition

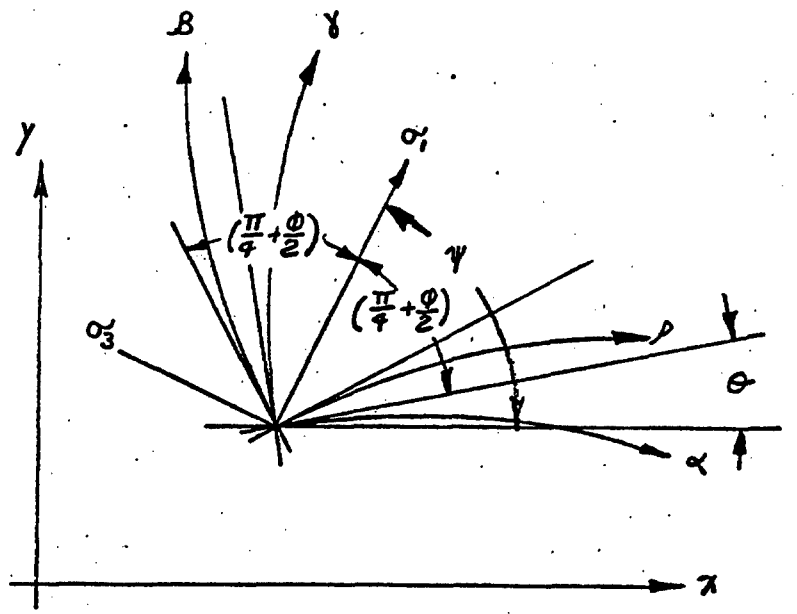

Figure 4. The α line and β line are characteristic curves of the stress equations. Either the α and γ lines or the ρ and β lines are the characteristic curves of the velocity equations.

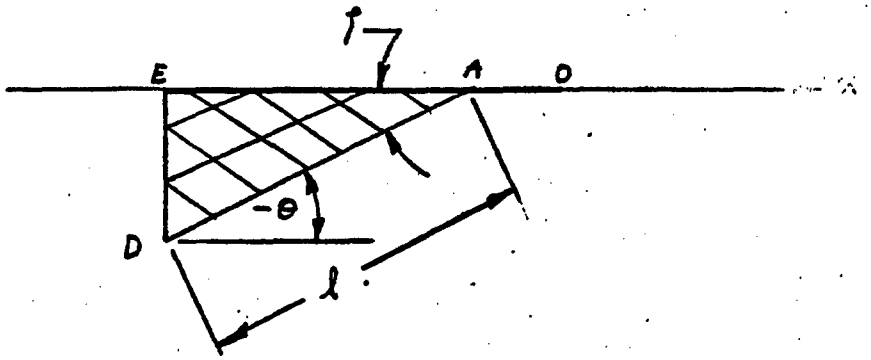

Figure 5(a). Stress Characteristic Field $\varphi = 30^{\circ}$, $\theta = -25^{\circ}$

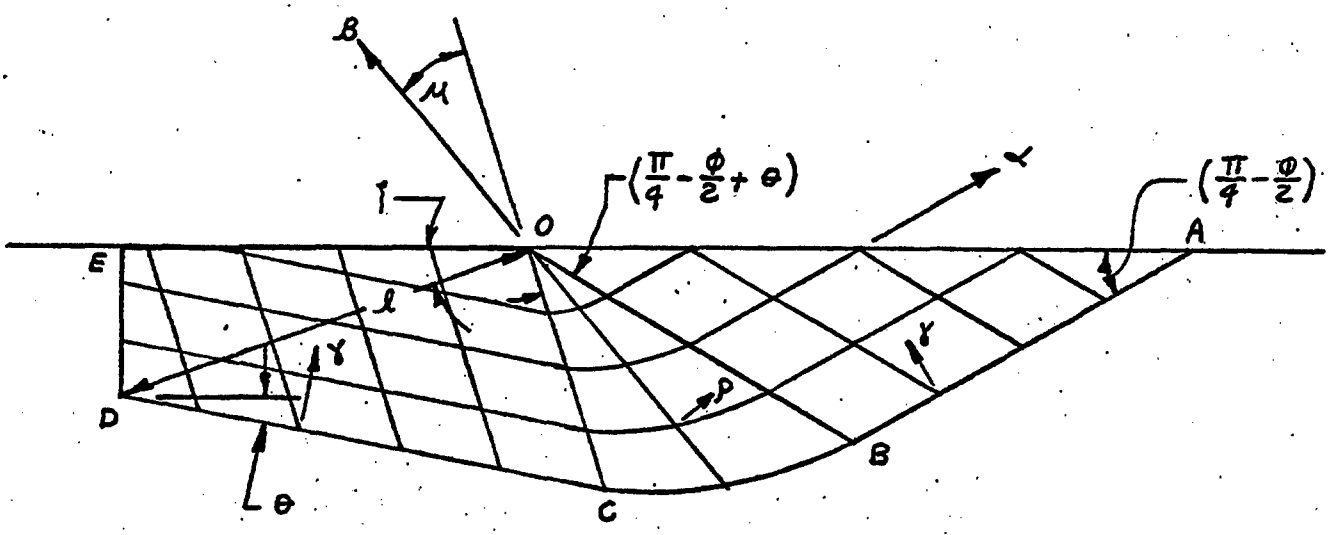

Figure 5(b). Stress Characteristic Field $\varphi = 30^{\circ}$, $\theta = 10^{\circ}$

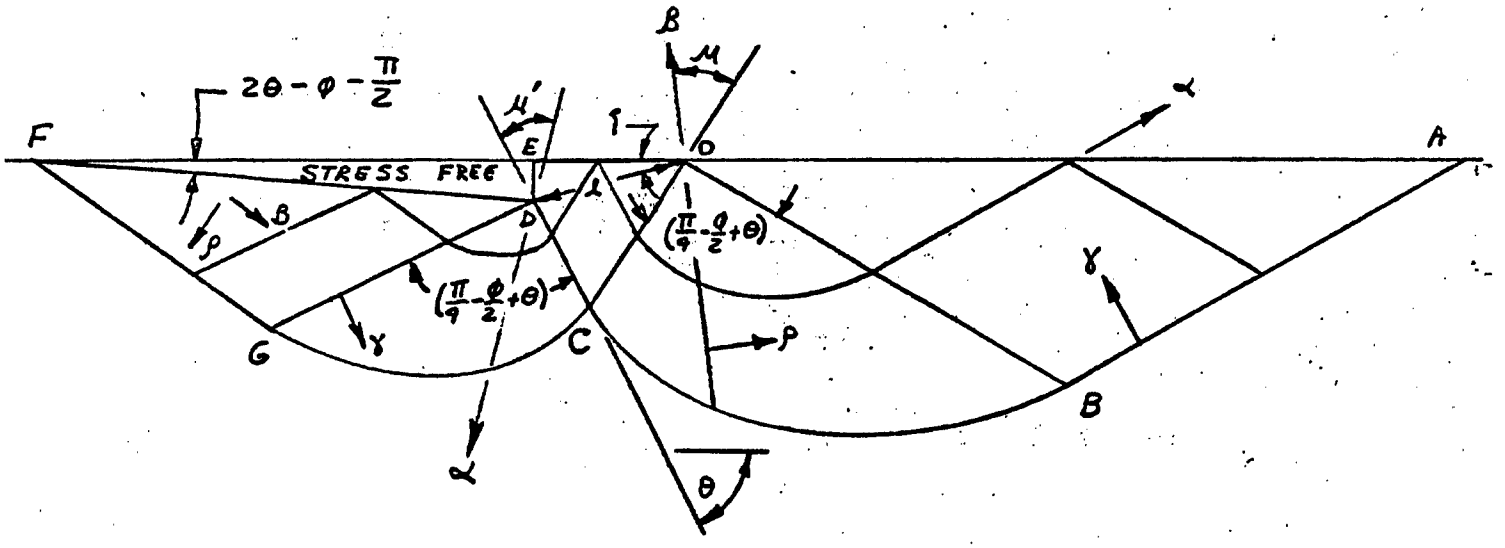

Figure 5(c). Stress Characteristic Field $\varphi = 30^\circ$, $\theta = 62^\circ$

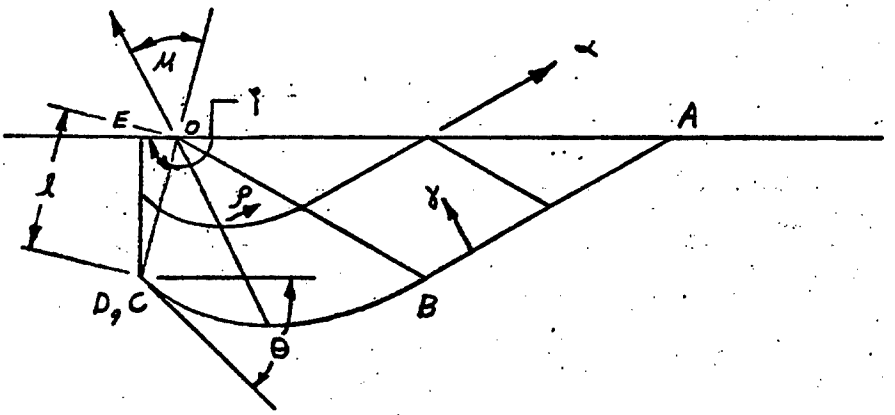

Figure 5(d). Stress Characteristic Field $\varphi = 30^\circ$, $\theta = 45^\circ$

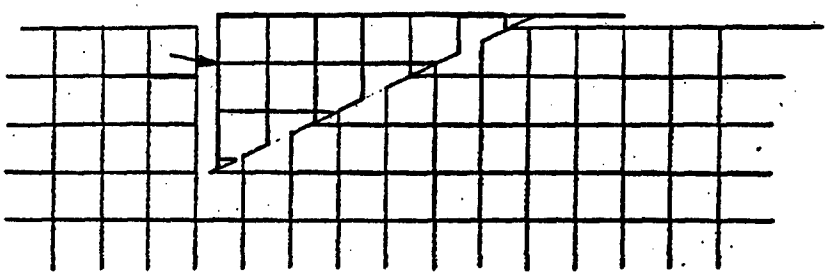

Figure 6(a). Configuration of Initially Square Grid after Small Plate Displacement $\varphi = 30^{\circ}$, $\theta = -25^{\circ}$

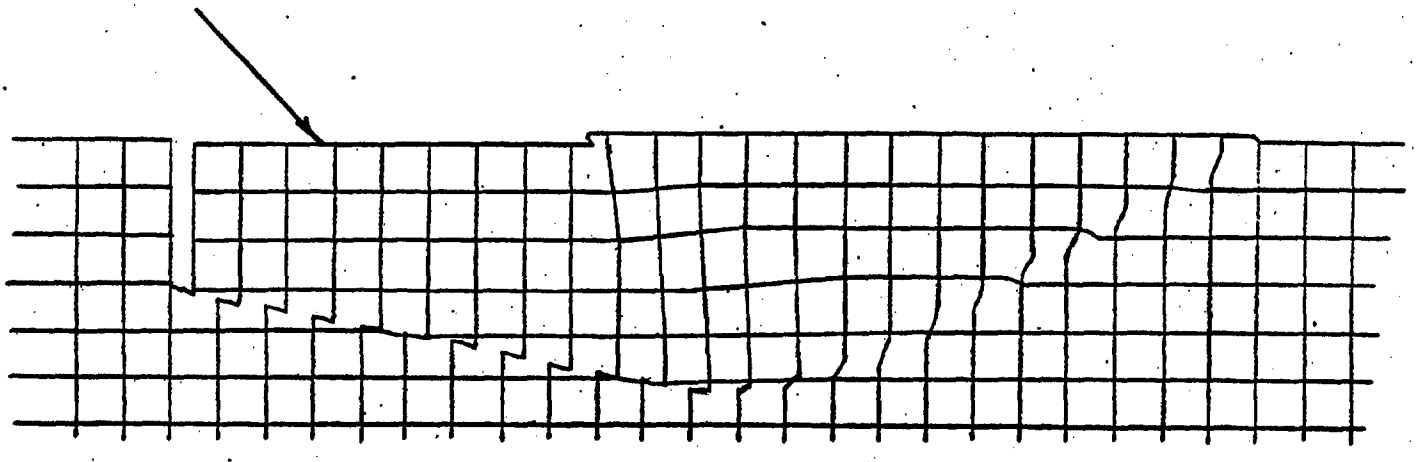

Figure 6(b). Configuration of Initially Square Grid after Small Plate Displacement $\varphi = 30^{\circ}$, $\theta = 10^{\circ}$

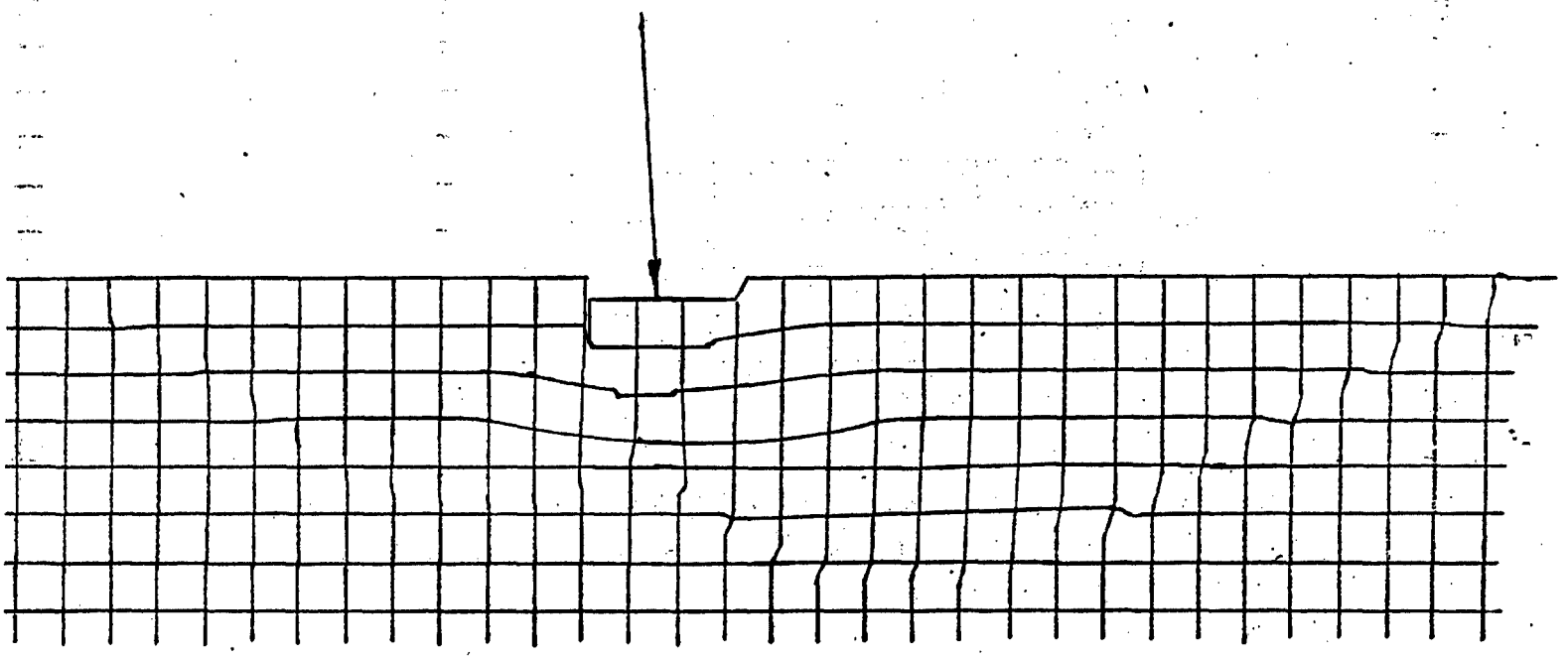

Figure 6(c). Configuration of Initially Square Grid after Small Plate Displacement $\varphi = 30^{\circ}$, $\Theta = 75^{\circ}$

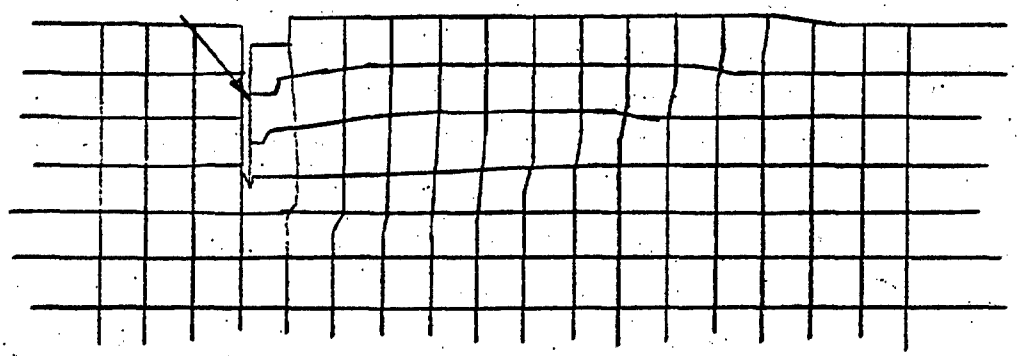

Figure 6(d). Configuration of Initially Square Grid after Small Plate Displacement $\varphi = 30^{\circ}$, $\Theta = 75^{\circ}$

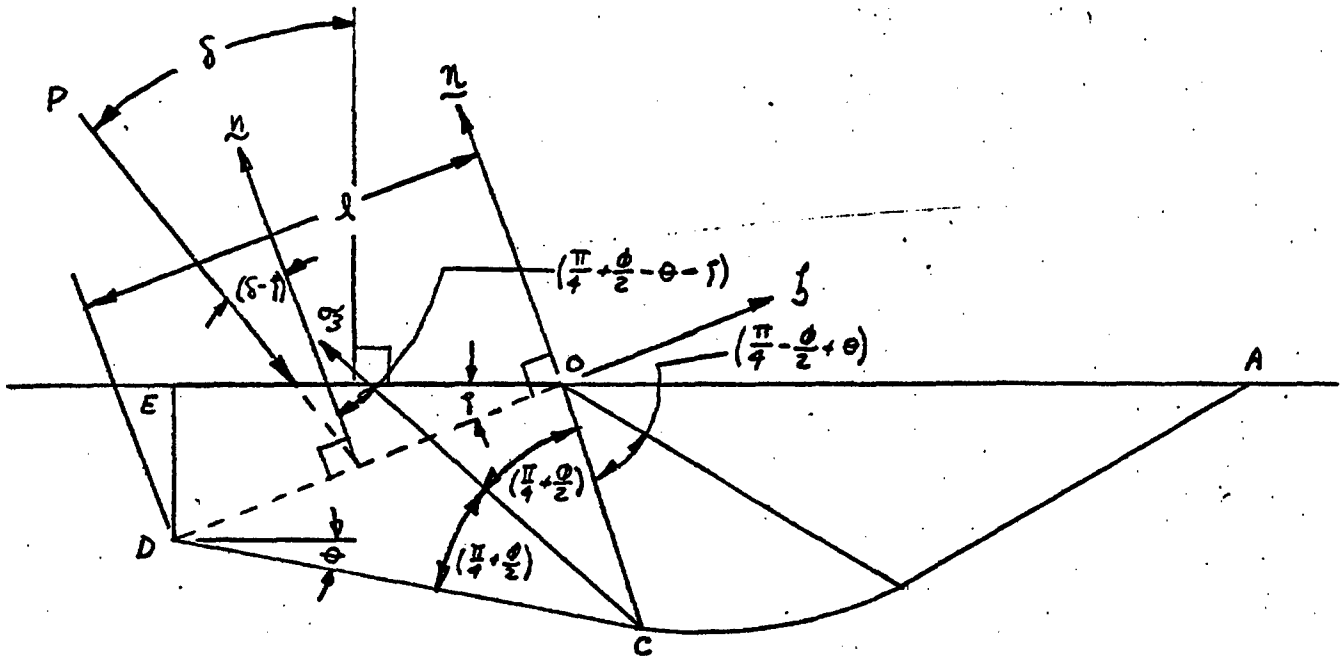

Figure 7(a). Plate Load and Stress Characteristic Field. The line of action of the plate load intersects the line OD at its midpoint.provided A lies to the right of 0 . If A lies to the left of 0 as in fig. 5(a), then the line AD is intersected at its midpoint by the plate load.

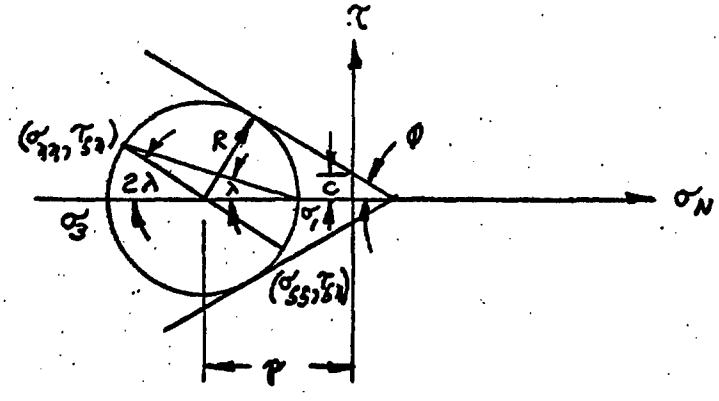

Figure 7(b). Mohr Diagram. $\lambda = \left(\frac{\pi}{4} + \frac{\varphi}{2} = 5\right)$

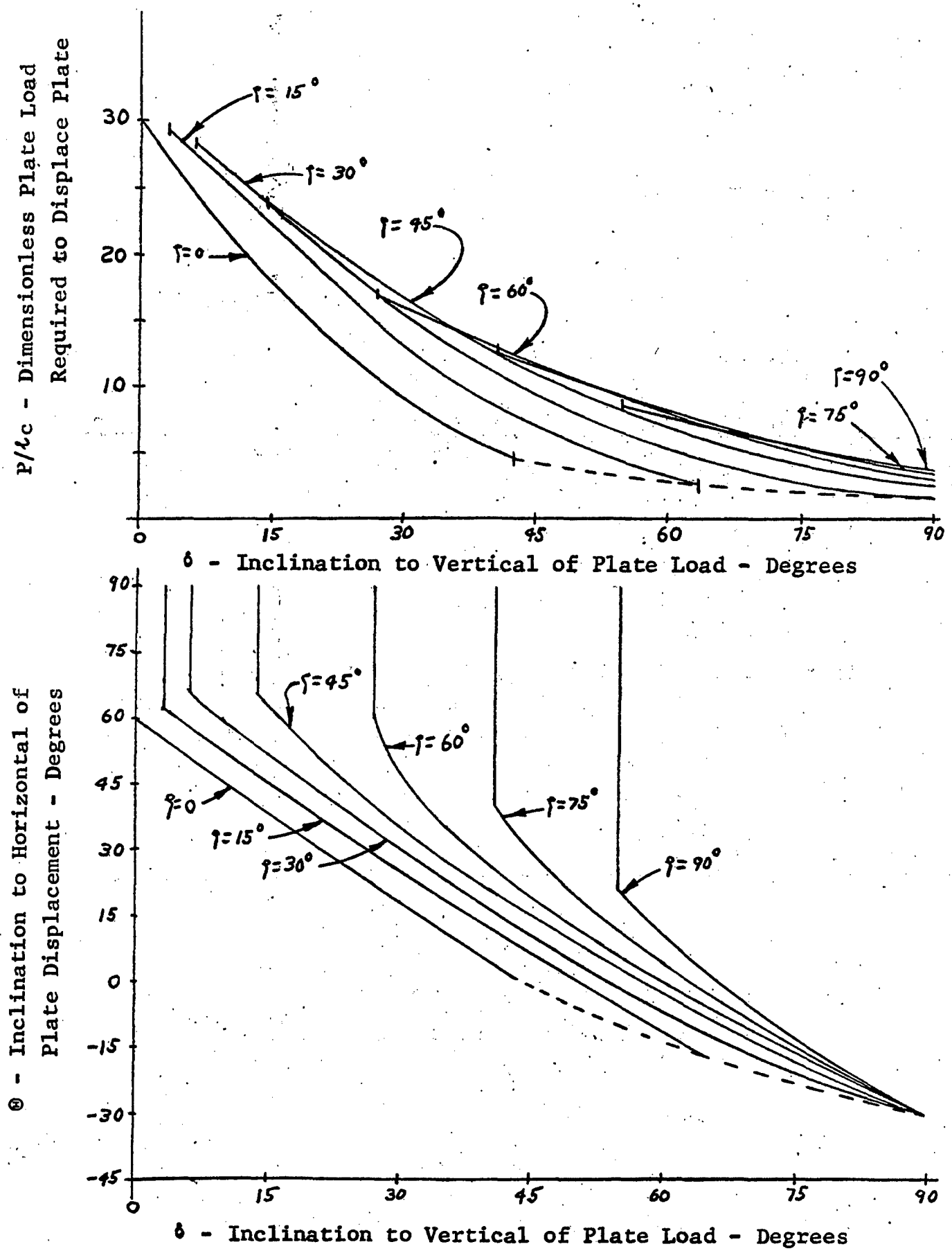

Figure 8. Plate Performance Curves - $\varphi = 30^{\circ}$

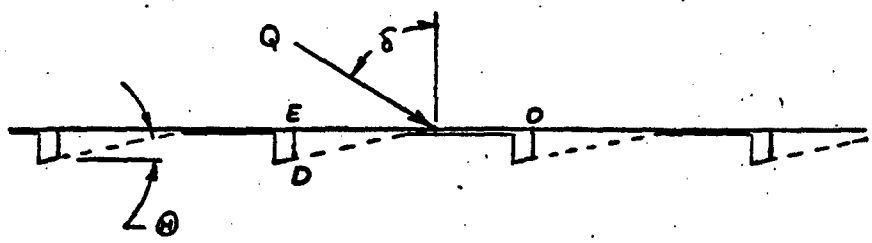

Figure 9. Section of Infinitely Long Plate with Equally Spaced Spuds of Uniform Depth Before and After Small Indentation

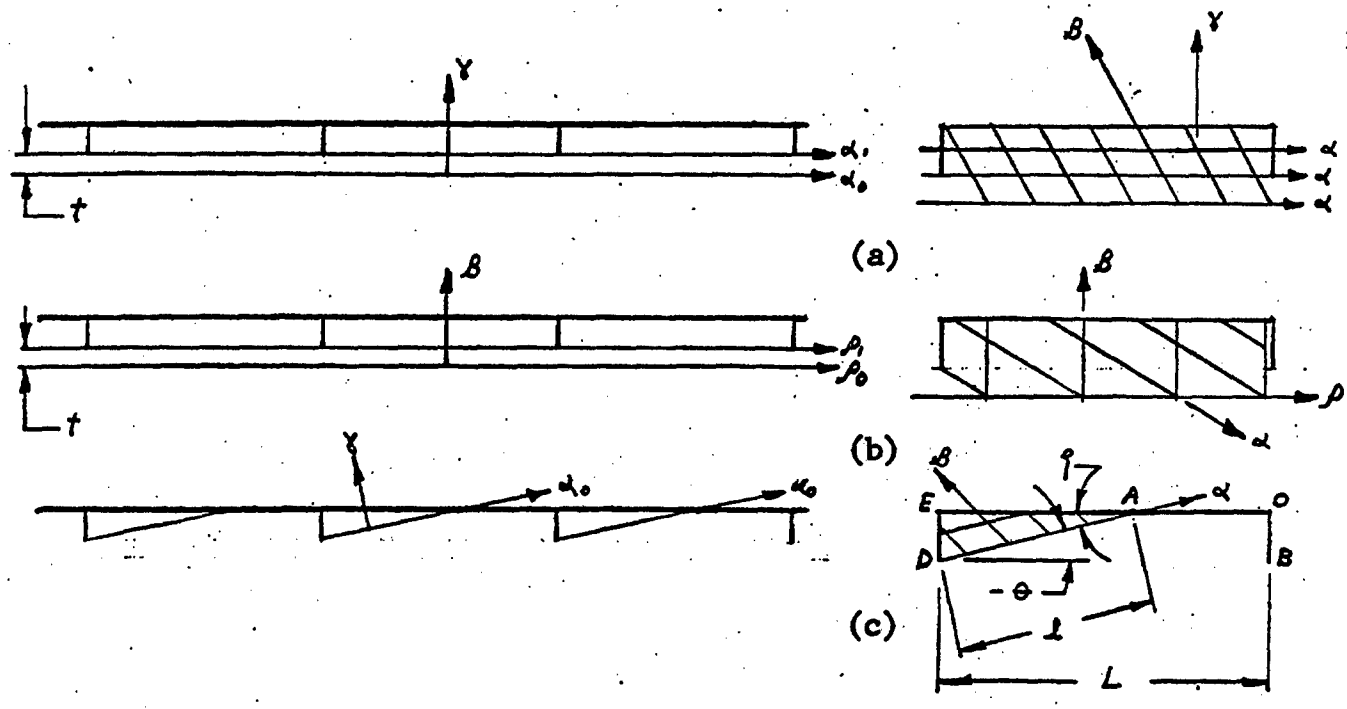

Figure 10. Alternative Characteristic Fields for Infinite Plate Problem. $\varphi = 30^{\circ}$

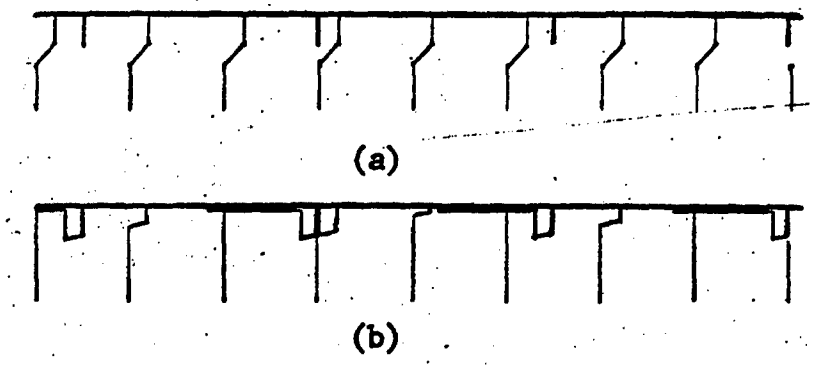

Figure 11. Configurations of Grids of Initially Vertical Lines. Fig. 11(a) corresponds to figs. 10(a) and 10(b). Fig. 11(b) corresponds to fig. 10(c).

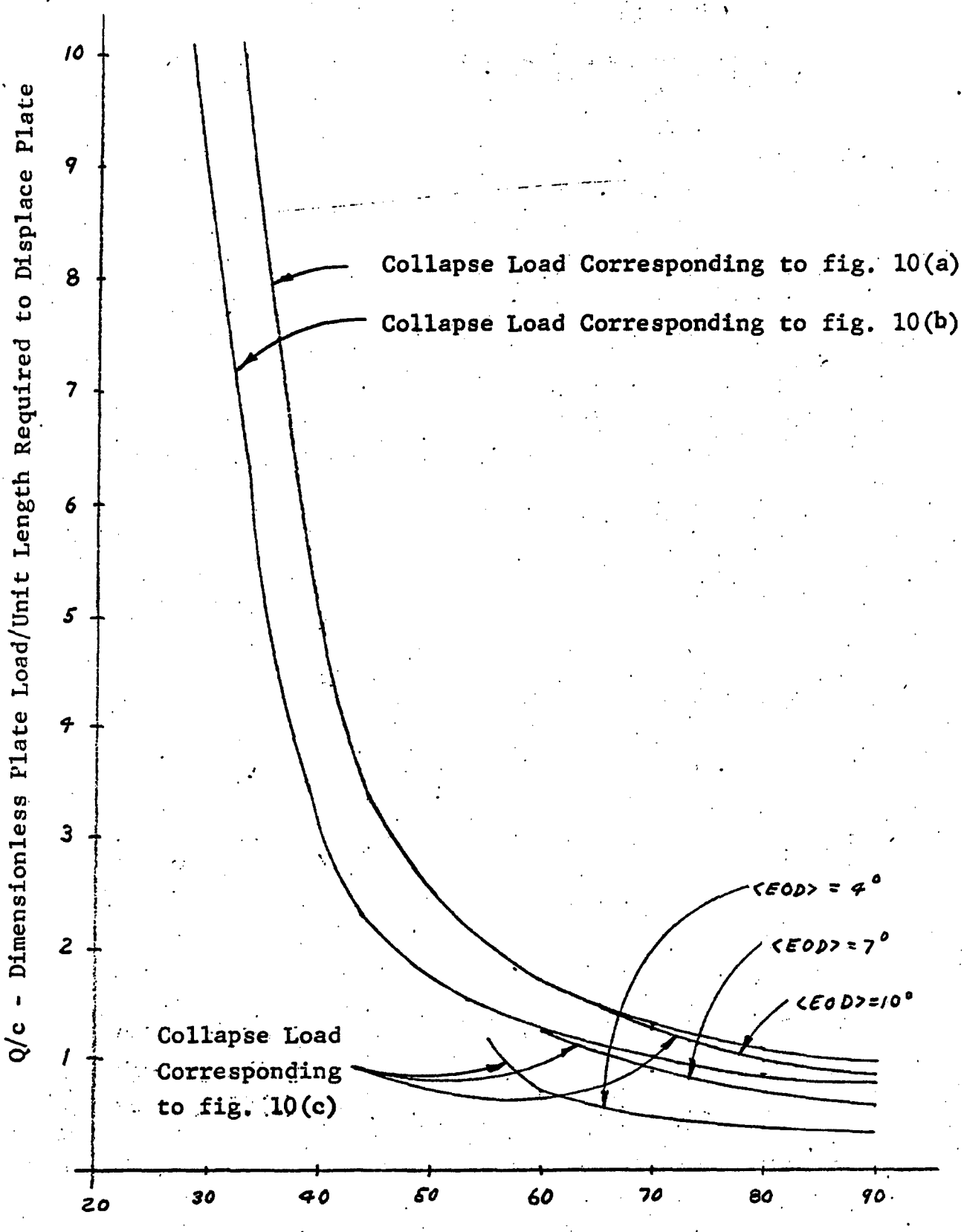

Figure 12. Collapse Loads for Infinite Plate. $\varphi = 30^{\circ}$

REFERENCES

1. Bekker, M. G., "Introduction to Research on Vehicle Mobility, Part I - Stability Problem", Ordnance Tank Automotive Command, Land Locomotion Research Branch Report No. 22.

2. Dais, J. L., "An Isotropic Frictional Theory for a Granular Medium With or Without Cohesion", Brown University, Technical Report No. NSF-GK1013/6, 1967.

3. Haythornthwaite, R. M., "Methods of Plasticity in Land Locomotion Studies", in "Rheologie et Mechanique des Sols", Proc. IUTAM Symposium, Grenoble, April 1964, edited by J. Kravtchenko and P. J. Sirieys, Springer, 1966, pp. 28-44.

4. Bekker, M. G., "Theory of Land Locomotion", The University of Michigan Press, 1956.

DISTRIBUTION LIST

Commanding General U.S. Army Tank-Automotive Command Warren, Michigan 48090 Attention:	No. of Copies
Chief Scientist/Technical Director of Laboratories, AMSTA-CL	1
Chief Engineer, AMSTA-CR	1
Director, Development & Engineering Directorate, AMSTA-R	1
Vehicular Components & Materials Laboratory, ATTN: General Support Branch, AMSTA-BSG	2
Vehicle Systems Division, AMSTA-RE	2
International Technical Programs Division, AMSTA-RI	1
Engineering Control Systems Division, AMSTA-RS	2
Systems Concept Division, AMSTA-RR	2
Maintenance Directorate, AMSTA-M	2
Quality Assurance Directorate, AMSTA-Q	2
Commodity Management Office, AMSTA-W	2
Vehicular Components & Materials Laboratory, ATTN: Research Library Branch, AMSTA-BSL	3
Safety & Reliability Division, AMSTA-RB	1
Land Locomotion Division, AMSTA-UL	10
Propulsion Systems Laboratory, AMSTA-G	5
Fire Power & Sub-System Integration Division, AMSTA-HF	1
Frame, Suspension & Track Division, AMSTA-UT	6
Scientific Computer Division, AMSTA-US	1
Technical Data Division, AMSTA-TD	2
Operations Support Division, AMSTA-RP	2
Combat Dev Comd Liaison Office, CDCLN-A	2
Marine Corp Liaison Office, USMC-LNO	2
Mobility Systems Laboratory, AMSTA-U	1
Canadian Army Liaison Office, CDLS(D)	2
USA EL Liaison Office, AMSEL-RD-MN	2
USA Weapons Comd Liaison Office, AMSWE-LCV	2
Reliability Engineering Branch, AMSTA-RTT	1
Sheridan Project Managers Office, AMCPM-SH-D	1
General Purpose Vehicles Project Managers Office, AMCPM-GP	1
M60, M60A1, M46A3 Project Managers Office, AMCPM-M60	1
Combat Veh Liaison Office, AMCPM-CV-D	1
US Frg MBT Detroit Office, AMCPM-MBT-D	1
XM561 Project Managers Office, AMCPM-GG	1

	No. of Copies
Commanding General U.S. Army Materiel Command Washington, D. C. ATTN: AMCRD-DM-G	2
Commander Defense Documentation Center Cameron Station Alexandria, Virginia 22314	20
Marry Diamond Laboratories ATTN: Technical Reports Group Washington, D. C.	1
U.S. Naval Civil Engineer Res & Engr Lab Construction Batallion Center Port Hueneme, California	1
Commanding General U.S. Army Test and Evaluation Command Aberdeen Proving Ground, Maryland ATTN: AMSTE-BB AMSTE-TA	1
Commanding General U.S. Army Supply & Maintenance Command Washington, D. C. 20310 ATTN: AMSSM-MR	1
Commanding General 18th Airborne Corps Fort Bragg, North Carolina 28307	1
Commanding General U.S. Army Alaska APO 409 Seattle, Washington	1
Office, Chief of Research & Development Department of the Army Washington, D. C.	2
U.S. Army Deputy Chief of Staff for Logistics Washington, D. C.	2

	No. of Copies
Commander U.S. Marine Corps Washington, D. C. Attention: AO-rH	1
Commanding Officer U.S. Army Aviation Material Labs Fort Eustis, Virginia Attention: TCREC-SDL	1
Commanding General U.S. Army General Equipment Test Activity Fort Lee, Virginia 23801 Attn: Transportation Logistics Test Directorate	1
Commanding General U.S. Army Medical Services Combat Development Agency Fort Sam Houston, Texas 78234	2
Commanding Officer Signal Corps Fort Monmouth, New Jersey 07703 ATTN: CSRDL	2
Commanding Officer Yuma Proving Ground Yuma, Arizona 85364 ATTN: STEYP-TE	1
Corps of Engineers U.S. Army Engineer Research & Development Labs Fort Belvoir, Virginia 22060	1
President U.S. Army Maintenance Board Fort Knox, Kentucky 40121	1
President U.S. Army Armor Board Fort Knox, Kentucky 40121	1
President U.S. Army Artillery Board Fort Sill, Oklahoma 73503	1
President U.S. Army Infantry Board Fort Benning, Georgia 31905	1

	No. of Copies
President U.S. Army Airborne Electronic & Special Warfare Board Fort Bragg, North Carolina 26307	1
President U.S. Army Arctic Test Center APO Seattle, Washington 98733	1
Director, Marine Corps Landing Forces Development Center Quantico, Virginia 22134	1
Commanding General Headquarters USARAL APO 949 Seattle, Washington ATTN: ARAOD	2
Commanding Officer Aberdeen Proving Ground, Maryland 21005 Attention: STEAP-TL	1
Commanding General U.S. Army Aviation School Office of the Librarian Fort Rucker, Alabama ATTN: AASPI-L	1
Plans Officer (Psychologist) PP&A Div, G3, Hqs, USACDCBC Fort ORD, California 93941	1
Commanding General Hq, U.S. Army Materiel Command Research Division Research and Development Directorate Washington, D. C. 20025	1
Canadian Army Staff 2450 Massachusetts Avenue Washington, D. C.	4
Commanding General U.S. Army Materiel Command ATTN: AMCRD-RV-E, Mr. Paul Carlton Washington, D. C. 20315	1

	No. of Copies
Director U.S. Army Engineer Waterways Experiment Station Corps of Engineers P.O. Box 631 Vicksburg, Mississippi 39181	3
Unit X Documents Expediting Project Library of Congress Washington, D. C. Stop 303	4
Exchange and Gift Division Library of Congress Washington, D. C. 20025	1
United States Navy Industrial College of the Armed Froces Washington, D. C. ATTN: Vice Deputy Commandant	10
Continental Army Command Fort Monroe, Virginia	1
Department of National Defense Dr. N. W. Morton Scientific Advisor Chief of General Staff Army Headquarters Ottawa, Ontario, Canada	1
Chief Office of Naval Research Washington, D. C.	1
Superintendent U.S. Military Academy West Point, New York ATTN: Prof. of Ordnance	1
Superintendent U.S. Naval Academy Annapolis, Maryland	1
Chief, Research Office Mechanical Engineering Division Quartermaster Research & Engineering Command Natick, Massachusetts	1

DOCUMENT CONTROL DATA - R&D

(Security classification of title, body of abstract and indexing annotation must be entered when the overall report is classified)

1. ORIGINATING ACTIVITY (Corporate author) Land Locomotion Division, AMSTA-UL	2a. REPORT SECURITY CLASSIFICATION UNCLASSIFIED 2b. GROUP

3. REPORT TITLE

Analysis of Soil Indentation by a Translating Grouser Plate

4. DESCRIPTIVE NOTES (Type of report and inclusive dates)

5. AUTHOR(S) (Last name, first name, initial)

Dais, J. L.

6. REPORT DATE	7a. TOTAL NO. OF PAGES	7b. NO. OF REFS
October 1968	30	4

8a. CONTRACT OR GRANT NO.	9a. ORIGINATOR'S REPORT NUMBER(S) 10278
b. PROJECT NO.	
c. AMCMS CODE: 5535.12.426	9b. OTHER REPORT NO(S) (Any other numbers that may be assigned this report)
d.	

10. AVAILABILITY/LIMITATION NOTICES

Each transmittal of this document outside the agencies of the U.S. Government must have prior approval of U.S. Army Tank-Automotive Command ATTN: AMSTA-BSL

11. SUPPLEMENTARY NOTES	12. SPONSORING MILITARY ACTIVITY
	Land Locomotion Division Mobility Systems Laboratory U.S. Army Tank-Automotive Command Warren, Michigan 48090

13. ABSTRACT

Soil is idealized as a weightless isotropic frictional material with cohesion, and quasi-static solutions are obtained to the two-dimensional problems of indentation by a plate with a single spud and an infinitely long plate with equally spaced spuds of uniform depth.

DD FORM 1 JAN 64 1473

14. KEY WORDS	LINK A		LINK B		LINK C	
	ROLE	WT	ROLE	WT	ROLE	WT
Spade indentation Spade holding ability Grousers						

INSTRUCTIONS

1. ORIGINATING ACTIVITY: Enter the name and address of the contractor, subcontractor, grantee, Department of Defense activity or other organization *(corporate author)* issuing the report.

2a. REPORT SECURITY CLASSIFICATION: Enter the overall security classification of the report. Indicate whether "Restricted Data" is included. Marking is to be in accordance with appropriate security regulations.

2b. GROUP: Automatic downgrading is specified in DoD Directive 5200.10 and Armed Forces Industrial Manual. Enter the group number. Also, when applicable, show that optional markings have been used for Group 3 and Group 4 as authorized.

3. REPORT TITLE: Enter the complete report title in all capital letters. Titles in all cases should be unclassified. If a meaningful title cannot be selected without classification, show title classification in all capitals in parenthesis immediately following the title.

4. DESCRIPTIVE NOTES: If appropriate, enter the type of report, e.g., interim, progress, summary, annual, or final. Give the inclusive dates when a specific reporting period is covered.

5. AUTHOR(S): Enter the name(s) of author(s) as shown on or in the report. Enter last name, first name, middle initial. If military, show rank and branch of service. The name of the principal author is an absolute minimum requirement.

6. REPORT DATE: Enter the date of the report as day, month, year, or month, year. If more than one date appears on the report, use date of publication.

7a. TOTAL NUMBER OF PAGES: The total page count should follow normal pagination procedures, i.e., enter the number of pages containing information.

7b. NUMBER OF REFERENCES: Enter the total number of references cited in the report.

8a. CONTRACT OR GRANT NUMBER: If appropriate, enter the applicable number of the contract or grant under which the report was written.

8b, 8c, & 8d. PROJECT NUMBER: Enter the appropriate military department identification, such as project number, subproject number, system numbers, task number, etc.

9a. ORIGINATOR'S REPORT NUMBER(S): Enter the official report number by which the document will be identified and controlled by the originating activity. This number must be unique to this report.

9b. OTHER REPORT NUMBER(S): If the report has been assigned any other report numbers *(either by the originator or by the sponsor)*, also enter this number(s).

10. AVAILABILITY/LIMITATION NOTICES: Enter any limitations on further dissemination of the report, other than those imposed by security classification, using standard statements such as:

(1) "Qualified requesters may obtain copies of this report from DDC."

(2) "Foreign announcement and dissemination of this report by DDC is not authorized."

(3) "U. S. Government agencies may obtain copies of this report directly from DDC. Other qualified DDC users shall request through _____."

(4) "U. S. military agencies may obtain copies of this report directly from DDC. Other qualified users shall request through _____."

(5) "All distribution of this report is controlled. Qualified DDC users shall request through _____."

If the report has been furnished to the Office of Technical Services, Department of Commerce, for sale to the public, indicate this fact and enter the price, if known.

11. SUPPLEMENTARY NOTES: Use for additional explanatory notes.

12. SPONSORING MILITARY ACTIVITY: Enter the name of the departmental project office or laboratory sponsoring *(paying for)* the research and development. Include address.

13. ABSTRACT: Enter an abstract giving a brief and factual summary of the document indicative of the report, even though it may also appear elsewhere in the body of the technical report. If additional space is required, a continuation sheet shall be attached.

It is highly desirable that the abstract of classified reports be unclassified. Each paragraph of the abstract shall end with an indication of the military security classification of the information in the paragraph, represented as *(TS), (S), (C), or (U)*.

There is no limitation on the length of the abstract. However, the suggested length is from 150 to 225 words.

14. KEY WORDS: Key words are technically meaningful terms or short phrases that characterize a report and may be used as index entries for cataloging the report. Key words must be selected so that no security classification is required. Idenfiers, such as equipment model designation, trade name, military project code name, geographic location, may be used as key words but will be followed by an indication of technical context. The assignment of links, rules, and weights is optional.